

A CW NORMAL CONDUCTING RF CAVITY FOR FAST CHIRP CONTROL IN THE LCLS-II

Mamdouh H. Nasr*, Paul J. Emma, Sami Tantawi
SLAC National Accelerator Laboratory, CA, USA

Abstract

We propose an RF chirping normal conducting (NC) linac structure to be located after the injector in the new LCLS-II under construction at SLAC. This chirping linac will provide peak current control of the FEL by adjusting the beam chirp at the zero-crossing phase rapidly from bunch to bunch. We examined standing wave (SW) and travelling wave (TW) linac designs spanning RF frequencies from L-band to X-band with each design optimized for minimum input RF power. For 20 mm iris diameter, an optimal design is found to be a SW linac structure operating at C-band with input RF power of only 10 kW. We also investigated smaller-diameter designs that can require only 500 W in case we can afford operating with such diameters from the wakefield point of view.

INTRODUCTION

The LCLS-II is a high repetition-rate Free-Electron Laser (FEL) facility under construction at SLAC. A new 4-GeV continuous wave (CW) superconducting (SC) L-band (1.3 GHz) linac is being built to provide an electron bunch rate of up to 1 MHz, with bunches rapidly switched between two FEL undulators. With different user groups on each FEL it is desirable to provide peak current (i.e., pulse length) control in each FEL independently by varying the RF phase (chirp) prior to the first bunch compressor. However, the high-Q, SCRF, with its 1-ms fill-time, cannot be changed within one bunch spacing (1 μ s) [1].

So to provide a small chirp adjustment from bunch to bunch, we propose a short CW copper RF accelerating cavity, located just after the injector, with < 250-ns fill-time designed specifically to adjust the beam chirp at either zero-crossing phase. At ± 1 MV in S-band, this small chirp adjustment is capable of doubling or halving the final pulse length (or in-between) rapidly from bunch to bunch. This would allow us to deliver a shot-to-shot variable pulse duration and peak current to the different FEL users on LCLS-II.

We examined RF cavity designs spanning RF frequencies from L-band to X-band. We considered both SW and TW structures. We found an optimal solution with 2 cm iris diameter, SW RF cavity, operating at C-band with input power of only 10 kW. If one can afford to operate with smaller diameter, from a wakefield point of view, then similar structure at X-band may require only 500 W with 5 mm iris diameter.

In the following sections, we will introduce the parameter guidelines for our chirping linac structure, then, briefly present the power calculation formulas for SW and TW linac

design as well as our design results, afterwards, the optimum design will be simulated to illustrate the provided peak current control, and finally, we will provide some insight on designs with smaller iris diameter.

DESIGN PARAMETER GUIDELINES

All the provided designs are short linacs with 1-meter length. The iris diameter, however, is chosen to be large (20 mm) to avoid unfavorable wakefield effects and to stay clear of high-power beam. A filling time of < 250-ns is chosen to be able to change the chirping value and/or polarity within two-consecutive bunch spacing (1 μ s). We also designed for maximum accelerating voltage of ± 1 MV at S-band, although the bunch will be phased on the zero-crossing in operation. For other bands, the accelerating voltage (ΔV) is scaled such that we maintain a constant-chirping slope. This can be satisfied for short bunches using the following relation [2]

$$\text{Chirping slope} \propto \frac{\Delta V}{\lambda} = \text{const.} \rightarrow \frac{\Delta V_1}{\lambda_1} = \frac{\Delta V_2}{\lambda_2} \quad (1)$$

with a reference value of $\Delta V = \pm 1$ MV at S-band ($f = 2.8562$ GHz).

SW LINAC POWER CALCULATION

We will start by the power balance expression for a general cavity

$$P_i = P_{r,tot} + P_{loss} + \frac{\partial U}{\partial t} \quad (2)$$

where, P_i is the input RF power to the cavity, $P_{r,tot}$ is the total reflected power at the cavity port, P_{loss} is the power loss to the cavity walls, and U is the stored energy inside the cavity.

The total reflected field $E_{r,tot}$ is defined as the summation of the reflected field (E_r) and the emitted field through the cavity port (E_e). As a result, $E_{r,tot} = E_r + E_e \approx -E_i + E_e$, where E_i is the incident field, assuming small port dimension that leads to large reflection.

We can derive the differential equation for $|E_e|$ from (2) by simply making use of the basic definition of the intrinsic quality factor of the cavity (Q_0) and the external one (Q_e) and substituting for the power in terms of field magnitudes, leading to the following equation

$$\frac{\partial |E_e|}{\partial t} + \frac{\beta + 1}{\tau} |E_e| = \frac{2\beta}{\tau} |E_i| \quad (3)$$

where $\beta = Q_0/Q_e$ and $\tau = 2Q_0/\omega_0$ with ω_0 is the resonance frequency of the cavity.

* mamdouh@slac.stanford.edu

We can solve (3) for a unit-step input to study the rising edge of $|E_e|$, which leads to the following expression

$$|E_e| = \frac{2\beta}{\beta + 1} \left(1 - \exp\left(-t \frac{\beta + 1}{\tau}\right) \right) \quad (4)$$

We defined the filling time (t_f) as the time required to reach 95% of the steady state value which leads to the condition that $\beta \approx -1 + 3 \frac{\tau}{t_f}$ with $t_f = 250$ ns i.e. we will control the external quality factor (Q_e) in order to satisfy the required filling time. At this stage, we can define the total reflection coefficient at the port (Γ), using the steady state value of the fields, as follows

$$\Gamma = \left| \frac{E_{r,tot}}{E_i} \right| = \left| \frac{E_e - E_i}{E_i} \right| \approx \left| 1 - 0.67 \frac{t_f}{\tau} \right| \quad (5)$$

Then, we can calculate the input RF power as follows

$$P_i = \frac{P_{loss}}{1 - \Gamma^2} \approx \frac{|\Delta V/L|^2 / r_s}{1 - \left| 1 - 0.67 \frac{t_f}{\tau} \right|^2} \quad (6)$$

where r_s is shunt impedance of the linac and $\Delta V/L$ is the average accelerating gradient.

TW LINAC POWER CALCULATION

It is not challenging to achieve a filling time of 250 ns for TW linac, thus we chose to operate with the $2\pi/3$ mode as it have the highest shunt impedance [3] which leads to low input RF power. The filling time for a travelling wave linac can simply be expressed as $t_f = \frac{L}{v_g}$ with L is the length of the structure and $v_g = \frac{\partial \omega}{\partial \beta}$ is the group velocity which can be obtained by differentiating the dispersion curve. For a TW constant-impedance linac, we can express the voltage gain (on-crest) using the following expression [4]

$$\Delta V = \sqrt{2r_s P_i L} \frac{1 - \exp(-\tau_0)}{\sqrt{\tau_0}}, \quad \tau_0 = \frac{\omega_0 L}{2Q_0 v_g} \quad (7)$$

As a result, we can express the input power as follows:

$$P_i = \frac{|\Delta V|^2 \tau_0}{2r_s L (1 - \exp(-\tau_0))^2} \quad (8)$$

SUMMARY OF RESULTS

We optimized the linac geometry to minimize the required input RF power at each band with the linac operating in π and $2\pi/3$ modes for SW and TW linacs, respectively. Table 1 shows the summary of results for our design at each band with iris diameter (D) of 20 mm.

From Table 1, we can initially expect that the X-band design is the optimum one as it utilizes the least input RF power among all the designs. However, further investigation shows that the X-band frequency exceeds the cut-off frequency of the cylindrical (20 mm diameter) guides that connect the consecutive linac cells. This will produce extremely large coupling between the cells that could excite multi-modes and

Table 1: Summary of Optimized SW and TW Designs for $D = 20$ mm

Band	f (GHz)	SW linac		TW linac	
		P_i (kW)	P_{loss} (kW)	P_i (kW)	P_{loss} (kW)
X	11.424	3.12	2.49	21.94	3.6586
C	5.711	10.73	5.07	17.29	8.706
S	2.856	70.57	15.85	54.33	13.02
L	1.3	904	81.05	Not realizable	

introduce many practical complications for such a design. We should also point out that the required filling time was not realizable for a TW linac at such a low frequency for L-band even for $\pi/2$ mode. Consequently, we chose the SW C-band design to be the optimum one. This design utilizes an input RF power of only 10 kW and power loss of only 5 kW. Figure 1 defines the geometry of one cell of our C-band SW optimized design and also shows the normalized field distribution.

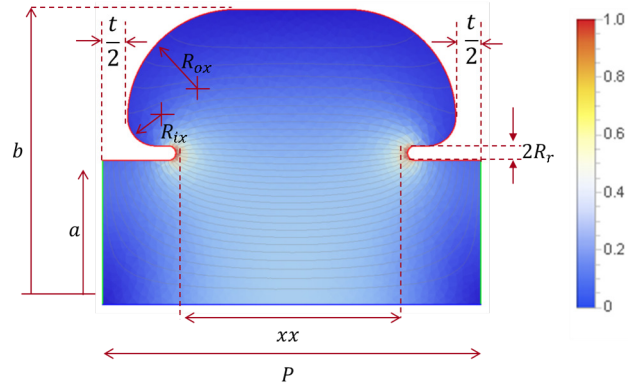


Figure 1: One cell of the optimized C-band SW design with $a=1$, $b=2.04247$, $P=2.62439$, $t=0.345$, $xx=1.61$, $R_{ox}=0.8975$, $R_{ix}=0.195$, $R_r=0.05$ cm.

ILLUSTRATION OF CHIRPING CONTROL

According to (1), the required accelerating voltage for our C-band SW linac is $\Delta V = \pm 0.5$ MV. This small chirp adjustment is capable of doubling or halving the final pulse length (or in-between) rapidly from bunch to bunch. The C-band SW NC linac is planned to be located before the first magnetic compressor in LCLS-II as illustrated in Fig. 2.

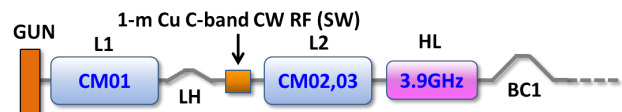


Figure 2: The intended location of the NC chirping linac in LCLS-II.

In the following, we will simulate the LCLS-II, with our NC chirping linac added to the system. These simulations are performed using the LiTrack fast longitudinal phase space tracking code [5]. Figure 3 shows the longitudinal phase space (left column) and the peak current profile (right column) of the electron beam. The fast chirper RF voltage is set to zero in the middle row of plots (a 1 kA peak current), to +0.5 MV on the top row of plots (a 2.5 kA peak current), and to -0.5 MV on the bottom row (a 600 A peak current). These profiles are taken at the start of the FEL undulator at 4 GeV. In all cases, the RF is set at the zero crossing phase, adding no acceleration, but chirping the electron bunch just prior to the first magnetic compressor chicane (BC1), which initiates the bunch length compression. The plots all have the same peak current and temporal scales for clarity.

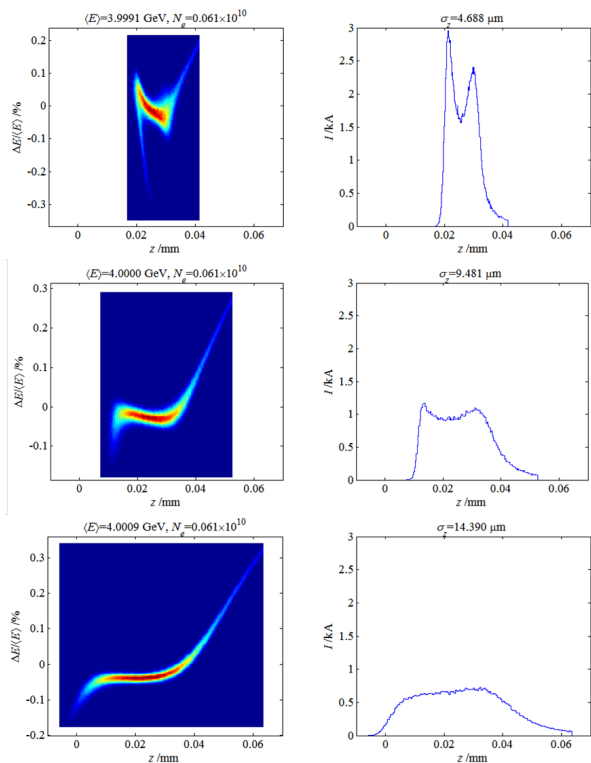


Figure 3: The longitudinal phase space (left column) and the peak current profile (right column) of the electron beam. The fast chirper RF voltage is set to zero in the middle row of plots, to +0.5 MV on the top row of plots, and to -0.5 MV on the bottom row.

SMALLER IRIS DIAMETER

As mentioned before, all the previously proposed SW and TW designs had a large iris diameter of 20 mm to avoid the unfavorable wakefield effects. In this section, we will briefly provide some insight on the possible designs for smaller iris diameter in case we can afford working with such structures from the wakefield point of view. We repeated our design

steps, but with the ratio of iris diameter to wavelength kept constant at 0.2. The latter optimization led to the results summarized in Table 2.

Table 2: Summary of Optimized SW and TW Designs for $D/\lambda = 0.2$

Band	f (GHz)	$\approx D$ (Cm)	SW linac		TW linac	
			P_i (kW)	P_{loss} (kW)	P_i (kW)	P_{loss} (kW)
X-band	11.424	0.5	0.487	0.445	0.6036	0.483
C-band	5.711	1	5.184	2.66	4.32	2.3
S-band	2.856	2	70.57	15.85	54.33	13.02
L-band	1.3	4	1531	117	1157	93

From the previous table we can see that, a SW structure at X-band may require only 500 W with 5 mm iris diameter. However, as mentioned, this will require further study of wakefields to make sure that one can afford to operate with such smaller diameter.

CONCLUSION

In this paper, we proposed a NC chirping linac structure that is intended to be located in LCLS-II under construction at SLAC. This chirping linac will provide peak current control and thus pulse width control for the FEL radiation. Different SW and TW designs were proposed operating at RF frequency spanning from L-band to X-band with optimized geometry to minimize the input RF power at each band. An optimum design was found to be a C-band SW linac which utilizes an input RF power of only 10 kW and power loss of only 5 kW. The LCLS-II system was simulated with our NC linac added to the system, showing the peak current control that is provided by our linac with the RF is set at the zero crossing phase. Finally, more designs with smaller iris diameter were discussed and was found to require input RF power as low as 500 W in case we can afford using them from the wakefield point of view.

REFERENCES

- [1] The LCLS-II design. [Online]. Available: https://portal.slac.stanford.edu/sites/lcls_public/lcls_ii/Pages/design.aspx
- [2] P. Emma, H. Loos, and C. Behrens, “Fast, absolute bunch length measurements in a linac using an improved rf-phasing method,” *SLAC-PUB-11035*.
- [3] A. Chao, H. Moser, and Z. Zhao, *Accelerator Physics, Technology and Applications*, 2004.
- [4] T. P. Wangler, *RF Linear Accelerators*. John Wiley & Sons inc., 1998.
- [5] K. L. F. Bane and P. Emma, “Litrack: A fast longitudinal phase space tracking code with graphical user interface,” in *Proceedings of the 2005 Particle Accelerator Conference*, May 2005, pp. 4266–4268.